

Probe Report

Title: Potent and selective inhibitors of NAD⁺-dependent 15-hydroxyprostaglandin dehydrogenase (HPGD)

Authors: Ajit Jadhav¹, Frank H. Niesen², Lena Schultz¹, Udo Oppermann², David J. Maloney¹, Anton Simeonov¹

¹NIH Chemical Genomics Center, 9800 Medical Center Dr., Bethesda, MD, 20892

²Structural Genomics Consortium, University of Oxford, UK

Version: #3

Date Submitted: March 2, 2011

Assigned Assay Grant #: 5U54MH084681 (U54 CDP)

Screening Center Name & PI: NIH Chemical Genomics Center, Christopher Austin

Chemistry Center Name & PI: NIH Chemical Genomics Center, Christopher Austin

Assay Submitter & Institution: Udo Oppermann, Structural Genomics Consortium, University of Oxford

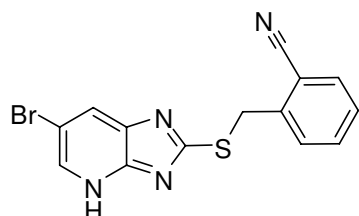
PubChem Summary Bioassay Identifier (AID): 2407

Abstract:

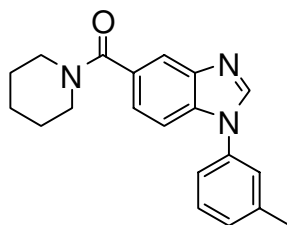
15-hydroxyprostaglandin dehydrogenase (15-PGDH; HPGD) is the key enzyme for the inactivation of prostaglandins, and thus regulates processes such as inflammation or proliferation. The anabolic pathways of prostaglandins are well-characterized, especially with respect to regulation of the cyclooxygenase (COX) enzymes. In comparison, little is known about downstream events, including functional interaction of prostaglandin-processing and metabolizing enzymes, as well as the function of prostaglandin receptors. To date, the only known strong inhibitors belong to the family of thiazolinedines that affect other pathways, notably by binding to peroxisome proliferator-activated receptor (PPAR) γ . The present study discloses the discovery and characterization of a potent and competitive HPGD inhibitor that is selective within the dehydrogenase family, ML147 (CID-3245059). It also discloses two high-affinity and uncompetitive HPGD inhibitors that are selective within the dehydrogenase family,

ML148 (CID-3243760) and ML149 (CID-2331284). These small molecule probes represent the most potent and selective inhibitors of 15-HPGD reported thus far.

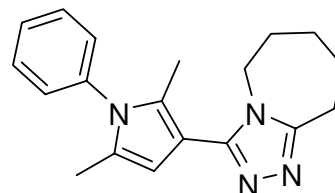
Probe Structure & Characteristics:



NCGC00044151-02
MLS002729015
CID 3245059
ML147



NCGC00065167-02
MLS002729014
CID 3243760
ML148



NCGC00037850-02
MLS002729013
CID 2331284
ML149

CID/ML#	Target Name	IC ₅₀ /EC ₅₀ (nM) [SID, AID]	Anti-target Name(s)	IC ₅₀ /EC ₅₀ (μM) [SID, AID]	Fold Selective	Secondary Assay(s) Name: IC ₅₀ /EC ₅₀ (nM) [SID, AID]
3245059/ ML147	HPGD	141.3nM [SID:8755071 7. AID: 2429	ALDH1A	> 57μM [SID:425136 0, AID: 1030	> 2000-fold	HPGD-deltaTm 12.2°C, [SID: 87550717; AID: 2427]
3243760/ ML148	HPGD	56.2nM [SID:8755071 8 AID: 2429	HADH2; HSD17β	> 57μM [SID:424987 7; AID: 886; 893]	> 1000-fold	HPGD-deltaTm 7.3°C, [SID: 87550718; AID: 2427]
2331284/ ML149	HPGD	89nM [SID:8755071 6AID: 2429	HADH2; HSD17β	> 57μM [SID:371764 2; AID: 886; 893]	> 1000-fold	HPGD-deltaTm 10.5°C, [SID: 87550716; AID: 2427]

Recommendations for scientific use of the probe:

Inhibition of 15-HPGD has been implicated as a viable target for the treatment of a variety of disorders, including dermal wound healing, bone formation and hair loss. In contrast, down-regulation of HPGD has been linked to increase incidence of several cancers, implying the potential value of HPGD activators in the treatment of cancer. Probes ML147, ML148, ML149

represent an important advancement to enable research focused on the elucidation of these various processes. They will serve as useful tools for exploration of biological function and intracellular interactions of 15-PGDH.



1 Introduction

Eicosanoids are arachidonic acid derivatives that comprise distinct functional classes like prostaglandins (PGs), lipoxins and leukotrienes; these bioactive fatty acids control a multitude of physiological functions including inflammation and differentiation. Dysregulation of the enzymes responsible for the generation and metabolism of active prostaglandins and lipoxins contributes to malignant transformation and progression in a variety of cancer types, such as breast, colon, lung and bladder cancers¹. The intracellular levels of prostaglandins are controlled mainly by the interplay between the cyclooxygenase enzymes (COX-1 and COX-2) on the one hand, and 15-hydroxy-prostaglandin dehydrogenase (15 PGDH) and other inactivating enzymes on the other. COX-1 and -2 are bifunctional enzymes that, through their fatty acid cyclooxygenase- and prostaglandin (PG) hydroxyperoxidase activities, ultimately catalyze the generation of prostaglandin H₂ (PGH₂) from arachidonic acid². The other prostaglandins are then generated and transformed into one another by several isomerases and synthases, producing, e.g., prostacyclin (PGI₂) or thromboxane A₂ (TX). The wide variety of effects of prostaglandins in many different cell types is explained with binding to a variety of mainly G protein-coupled receptors, eleven of which are currently known³, but to some extent also to nuclear hormone receptors; direct transcriptional effects are thus elicited.

15-PGDH represents the key enzyme in the inactivation of a number of active prostaglandins, leukotrienes and hydroxyeicosatetraenoic acids (HETEs) (e.g. by catalyzing oxidation of PGE₂ to 15-keto-prostaglandin E₂, 15k-PGE)⁴. The human enzyme is encoded by the HPGD gene and consists of a homodimer with subunits of a size of 29 kDa. The enzyme was purified from human placenta and its primary structure determined by Edman degradation. It was subsequently cloned and characterized⁵. The enzyme belongs to the evolutionarily conserved superfamily of short-chain dehydrogenase/reductase enzymes (SDRs), and according to the recently approved nomenclature for human enzymes, it is named SDR36C1. Thus far, two forms of 15-PGDH have been identified, NAD⁺-dependent type I 15-PGDH and the type II NADP-dependent 15-PGDH,

also known as carbonyl reductase 1 (CBR1, SDR21C1). However, the preference for NADP and the high K_m values of CBR1 for most PGs suggest that the majority of the *in vivo* activity can be attributed to type I 15-PGDH⁴.

The exact role of 15-PGDH in the regulation of prostaglandin pharmacology remains unclear; however, recent studies suggest that in addition to finding inhibitors of 15-PGDH, discovery of activators could be therapeutically valuable. Markowitz and co-workers showed that there was an increase in the incidence of colon tumors in 15-PGDH knockout mouse models⁶. Moreover, Nakagawa and co-workers demonstrated that the onco-protein hypoxia-inducible factor 1- α stimulates prostaglandin E synthase in primary tumors, which when coupled with HPGD downregulation, provides a selective growth advantage in hypoxic conditions. A more recent study by Grammas and co-workers implicates increased HPGD expression in the protection of thrombin-mediated cell death⁷. It is well-known that HPGD is responsible for the inactivation of PGE₂, which is a downstream product of COX-2 metabolism. Moreover, PGE₂ has been found to be neurotoxic both *in vitro* and *in vivo*; thus COX-2 specific inhibitors, which decrease PGE₂ release, exhibit neuroprotective effects. While these studies suggest a need for activators of HPGD, the dearth of potent and selective small molecule inhibitors of HPGD make it difficult to conclude whether these effects correlate to orthogonal activities or the primary inactivation of prostaglandins.

Prostaglandin E (PGE₂) has also been shown to be beneficial in a variety of biological processes such as hair density⁸, dermal wound healing⁹, and bone formation¹⁰, which suggests that inhibitors of 15-HPGD represent a viable therapeutic strategy. Accordingly, to identify novel high-affinity inhibitors that may be used to explore the biological function and intracellular interactions of 15-PGDH, we performed a high-throughput screen (qHTS) of the MLSMR by using an *in vitro* enzymatic assay following the HPGD activity in real time kinetic mode by recording the fluorescence of the NADH cofactor reaction product.

2 Materials and Methods

Unless otherwise stated, all reactions were carried out under an atmosphere of dry argon or nitrogen in dried glassware. Indicated reaction temperatures refer to those of the reaction bath, while room temperature (rt) is noted as 25°C. All solvents were of anhydrous quality, purchased from Aldrich Chemical Co. and used as received. Commercially available starting materials and reagents were purchased from Aldrich and were used as received.

Analytical thin layer chromatography (TLC) was performed with Sigma Aldrich TLC plates (5x 20cm, 60 Å, 250µm). Visualization was accomplished by irradiation under a 254 nm UV lamp. Chromatography on silica gel was performed using forced flow (liquid) of the indicated solvent system on Biotage KP-Sil pre-packed cartridges and the Biotage SP-1 automated chromatography system. ¹H- and ¹³C NMR spectra were recorded on a Varian Inova 400 MHz spectrometer. Chemical shifts are reported in ppm with the solvent resonance as the internal standard (CDCl₃ 7.26 ppm, 77.00 ppm, DMSO-*d*₆ 2.49 ppm, 39.51 ppm for ¹H, ¹³C respectively). Data are reported as follows: chemical shift, multiplicity (s = singlet, d = doublet, t = triplet, q = quartet, br = broad, m = multiplet), coupling constants, and number of protons. Low resolution mass spectra (electrospray ionization) were acquired on an Agilent Technologies 6130 quadrupole spectrometer coupled to the HPLC system. High resolution mass spectral data were collected in-house using an Agilent 6210 time-of-flight mass spectrometer, also coupled to an Agilent Technologies 1200 series HPLC system. If needed, products were purified via a Waters semi-preparative HPLC equipped with a Phenomenex Luna[®] C18 reverse phase (5 micron, 30x 75mm) column having a flow rate of 45 ml/min. The mobile phase was a mixture of acetonitrile (0.025% TFA) and H₂O (0.05% TFA), and the temperature was maintained at 50°C.

Samples were analyzed for purity on an Agilent 1200 series LC/MS equipped with a Luna[®] C18 reverse phase (3 micron, 3x 75mm) column having a flow rate of 0.8-1.0 ml/min over a 7-minute gradient and a 8.5 minute run time. Purity of final compounds was determined to be >95%, using a 3µl injection with quantitation by AUC at 220 and 254 nm (Agilent Diode Array Detector).

2.1 Assays

qHTS Assay for Inhibitors of 15-PGDH (15-Hydroxyprostaglandin Dehydrogenase):

Inhibition of 15-PGDH (HPGD) activity was screened by utilizing prostaglandin as an electron donor and NAD^+ as an electron acceptor/cofactor. An increase in the fluorescence intensity due to conversion of NAD^+ to NADH was used to measure the enzyme activity. All compounds were screened using a qHTS approach, where compounds are assayed using at least seven concentrations to generate concentration-response curves for every compound. The methodology for creating a concentration-titration series between successive copies of library plates for the purpose of large-scale titration-based screening has been described¹¹. Briefly, qHTS uses an inter-plate dilution method where the first plate contains the highest concentration of a set of compounds in DMSO, while subsequent plates contain the same compounds in the same well locations, but at successive lower concentrations. Three μl of enzyme (20nM final concentration) were dispensed to 1536-well Greiner black solid bottom plates. Compounds (23nl) were transferred via Kalypsys PinTool. The plates were incubated for 15 min at room temperature, and then 1 μl of substrate/cofactor solution (Substrate/cofactor solution: 1mM NAD^+ and 30 μM prostaglandin (Sigma, prostaglandin E2, #P5640)) were added to start the reaction. The plates were immediately transferred to and read 4 times every 30 seconds on a ViewLux High-throughput CCD imager (Perkin-Elmer) using 340 nm excitation and 450 nm emission fluorescence protocol. The fluorescence intensity difference between the last and the first time points, normalized against controls, was used to compute reaction progress. Pubchem AID: 894

Confirmatory assay: The primary qHTS protocol described above was run against the follow-up confirmatory compounds. The confirmatory screen was run as a 24-point dilution series, and most of the 89 samples confirmed their qHTS activity. Pubchem AID: 2429.

Aldehyde dehydrogenase 1: (ALDH1A1) catalyzes the NAD^+ dependent oxidation of a variety of endogenous and exogenous aldehydes to the corresponding carboxylic acids. The enzyme is the critical step in the metabolic activation of retinoic acid, which plays an essential role as a nuclear receptor ligand. Furthermore, the precursor, retinaldehyde, has recently been shown to play a fundamental role in adipogenesis and obesity, which makes inhibitor development a possible target in metabolic diseases. ALDH1A1 shares some homology with HPGD, and it served as a suitable anti-target of HPGD to determine chemical probe selectivity. The assay

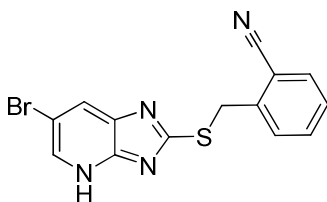
system is similar to the HPGD primary screening protocol. Inhibition of ALDH1A1 activity was screened by utilizing propionaldehyde as an electron donor and NAD^+ as an electron acceptor/cofactor. An increase in the fluorescence intensity due to conversion of NAD^+ to NADH was used to measure the enzyme activity. Pubchem AID: 1030.

Anti-target assays (HADH2 and HSD17 β 4): Two structurally related dehydrogenases were chosen as suitable anti-targets for characterizing selectivity of the probe series: HADH2 and HSD17 β 4. The mitochondrial enzyme 17-hydroxysteroid dehydrogenase type 10 (HSD17-10), previously classified as type II hydroxyacyl-CoA dehydrogenase (HADH2), catalyzes the NAD^+ -dependent oxidation of a variety of substrates including acyl-CoAs, androgens and neurosteroids, as well as bile acids. The role of HADH2 in neurodegeneration by binding to amyloid-peptide led to its identification, and mutations in its gene appear to be causative for 2-methyl-3-hydroxybutyryl-CoA dehydrogenase deficiency. HSD17 β 4 (17-beta-estradiol Dehydrogenase) is involved in peroxisomal fatty acid beta-oxidation.

The assay system for both anti-targets was similar to the HPGD primary screening protocol. Inhibition of HADH2 and HSD17 β 4 activity was screened by utilizing an electron donor (beta-hydroxybutyryl coenzyme A for HADH2 and estradiol for HSD17 β 4) as an electron donor and NAD^+ as an electron acceptor/cofactor. An increase in the fluorescence intensity due to conversion of NAD^+ to NADH was used to measure the enzyme activity. Pubchem AIDs: 886 and 893.

2.2 Probe Chemical Characterization

ML147:



Probe Characterization (NCGC00044151-02/CID:3245059/MLS002729015/ML147):

*Purity >95% as judged by LC/MS and ^1H NMR

2-((6-bromo-4H-imidazo[4,5-b]pyridin-2-ylthio)methyl)benzonitrile (ML147, CID: 3245059). ¹H NMR (400 MHz, DMSO-*d*₆) δ 4.76 (s, 2H), 7.48 (t, 1H, *J* = 7.5 Hz), 7.66 (t, 1H, *J* = 7.6 Hz), 7.71 (m, 1H), 7.86 (d, 1H, *J* = 7.6 Hz), 8.13 (brs, 1H), 8.30 (d, 1H, *J* = 1.6 Hz) and 13.37 (brs, 1H); HRMS: *m/z* (M)⁺ = 343.9732 (calculated for C₁₄H₉BrN₄S = 343.9731).

LC/MS conditions:

LC/MS (Agilent system) Retention time *t*₁ (short) = **3.43** min and *t*₂ (long) = **5.28**.

Column: 3 x 75 mm Luna C18, 3 micron

Run time: 4.5 min (short); 8.5 min (long)

Gradient: 4 % to 100 %

Mobile phase: Acetonitrile (0.025 % TFA), water (0.05 % TFA).

Flow rate: 0.8 to 1.0 mL

Temperature: 50°C

UV wavelength: 220 nm, 254 nm

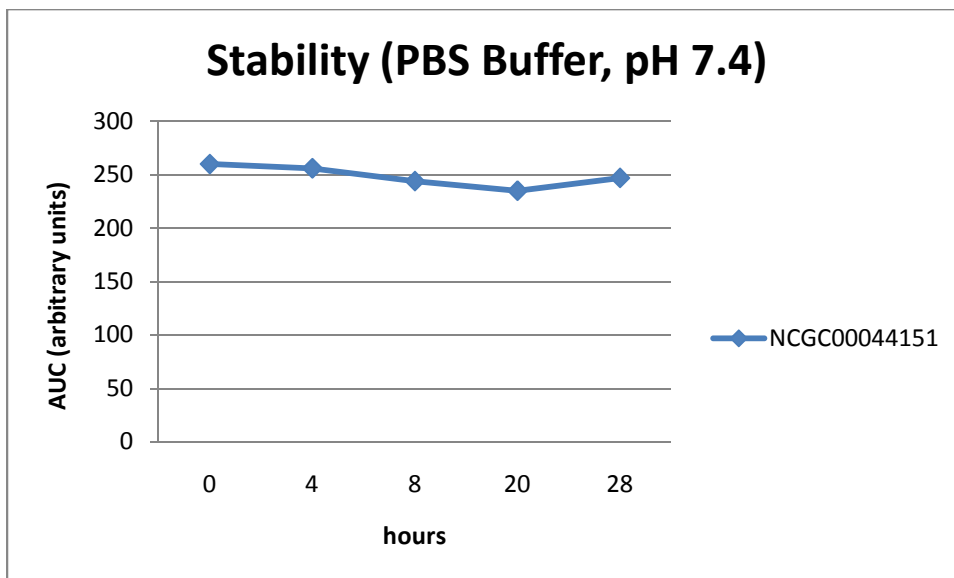
MLS numbers for probe analogues:

MLS IDs	SID	CID	ML
MLS002729015	99495751	3245059	*Probe compound ML147
MLS000533677	14746455	882270	
MLS000533691	14739715	708453	
MLS000041235	864287	665534	
MLS000557909	14742792	2039561	
MLS000527770	14725914	573334	

Probe *in vitro* ADME properties:

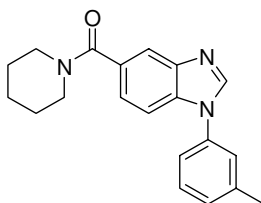
Aqueous (kinetic) solubility in PBS buffer (pH 7.4 @ 25 °C): 3μM

Experimental LogD: 2.35



Buffer Stability (48 h at 25°C) of (NCGC00044151-02/CID:3245059/MLS002729015), Percent remaining after 48h = 100%:

ML148:



Probe Characterization (NCGC00065167-02/CID:3243760/MLS002729014/ML148):

*Purity >95% as judged by LC/MS and ¹H NMR

Piperidin-1-yl(1-m-tolyl-1H-benzo[d]imidazol-5-yl)methanone-(ML148, CID: 3243760). ¹H NMR (400 MHz, DMSO-d₆) δ 1.3-1.65 (m, 6 H), 2.43 (s, 3H), 3.47 (brs, 4 H), 7.22-7.40 (m, 2 H), 7.40-7.59 (m, 3 H), 7.65 (d, 1H, *J* = 8.4 Hz), 7.75 (s, 1 H) and 8.62 (s, 1 H); HRMS: *m/z* (M+H)⁺ = 320.1768 (calculated for C₂₀H₂₂N₃O = 320.1763).

LC/MS conditions:

LC/MS (Agilent system) Retention time t_1 (short) = **3.15** min and t_2 (long) = **4.60**.

Column: 3 x 75 mm Luna C18, 3 micron

Run time: 4.5 min (short); 8.5 min (long)

Gradient: 4 % to 100 %

Mobile phase: Acetonitrile (0.025 % TFA), water (0.05 % TFA).

Flow rate: 0.8 to 1.0 mL

Temperature: 50°C

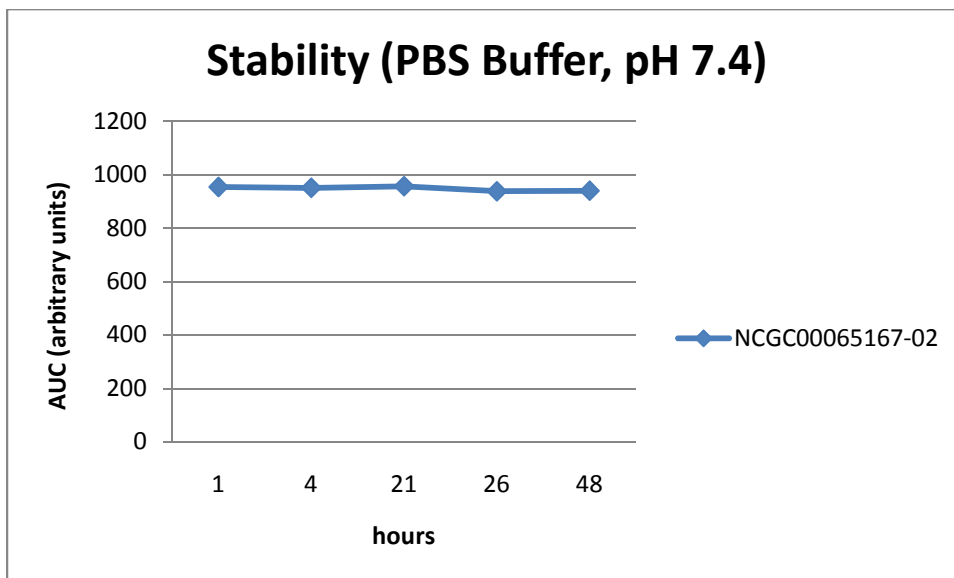
UV wavelength: 220 nm, 254 nm

MLS numbers for probe analogues:

MLS IDs	SID	CID	ML
MLS002729014	99495750	3243760	*Probe compound ML148
MLS000058178	3716805	2999763	
MLS000047077	4244157	3238792	
MLS000047085	4250491	3244293	
MLS000047086	4247671	3241847	
MLS000046502	4251412	3245103	

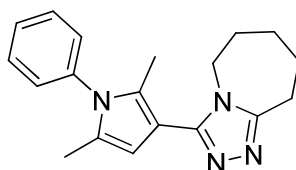
Probe *in vitro* ADME properties:

Compound	aq. Kinetic sol. (PBS @ pH 7.4)	Caco-2 (P_{app} 10^{-6} m/s @ pH 7.4)	efflux ratio (B→A)/ (A→B)	mouse liver microsome stability ($T_{1/2}$)	PBS-pH 7.4 Stability: % remaining after 48h	Mouse plasma stability: % remaining after 48h
NCGC00065167/ CID:3243760/ ML148	3 μ M	15	0.53	< 10min.	100	98



Buffer Stability (48 h @ 25°C) of (NCGC00065167/CID:3243760/MLS002729014/ML148), Percent remaining after 48h = 100%:

ML149:



Probe Characterization (NCGC00037850-02/CID:2331284/MLS002729013/ML149):

*Purity >95% as judged by LC/MS and ¹H NMR

3-(2,5-dimethyl-1-phenyl-1H-pyrrol-3-yl)-6,7,8,9-tetrahydro-5H-[1,2,4]triazolo[4,3-a]azepine (CID: 2331284). ¹H NMR (400 MHz, DMSO-d₆) δ 1.62-1.68 (m, 4 H), 1.80 (m, 2 H), 2.01 (s, 6 H), 2.91 (m, 2 H), 4.01 (m, 2 H), 6.02 (s, 1 H), 7.36 (d, 2H, *J* = 7.4 Hz) and 7.44-7.60 (m, 3 H); HRMS: *m/z* (M)⁺ = 306.1851 (calculated for C₁₉H₂₂N₄ = 306.1844).

LC/MS conditions:

LC/MS (Agilent system) Retention time *t*₁ (short) = **3.08** min and *t*₂ (long) = **4.34**.

Column: 3 x 75 mm Luna C18, 3 micron

Run time: 4.5 min (short); 8.5 min (long)

Gradient: 4 % to 100 %

Mobile phase: Acetonitrile (0.025 % TFA), water (0.05 % TFA).

Flow rate: 0.8 to 1.0 mL

Temperature: 50 °C

UV wavelength: 220 nm, 254 nm

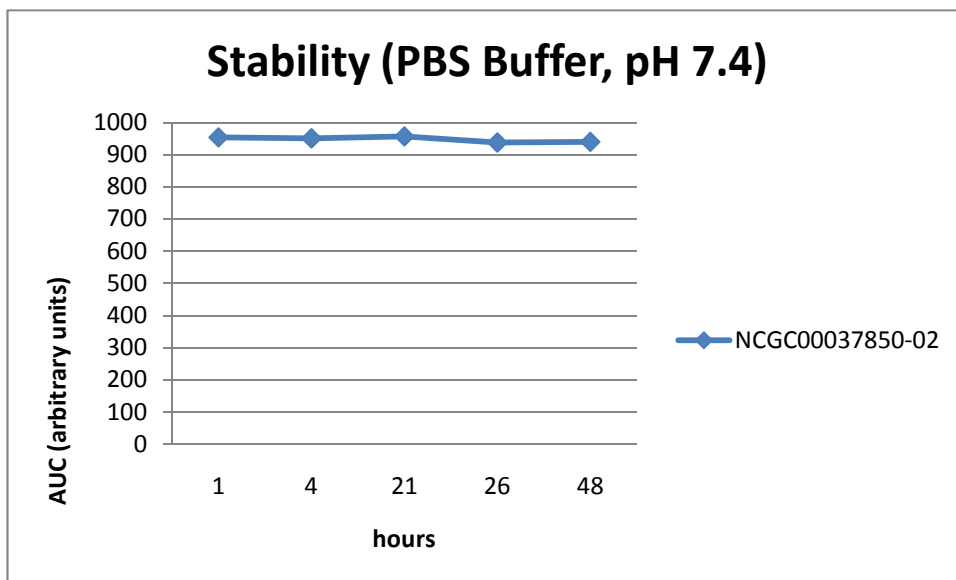
MLS numbers for probe analogues:

MLS IDs	SID	CID	ML
MLS002729013	3717642	2331284	*Probe compound ML149
MLS000053769	3711888	2997804	
MLS000097748	3713175	2120850	
MLS000335205	22407945	2089578	
MLS000567763	16952888	2523478	
MLS000390880	22405790	2359122	

Probe *in vitro* ADME properties:

Compound	aq. Kinetic sol. (PBS @ pH 7.4)	Caco-2 (P_{app} 10^{-6} m/s @ pH 7.4)	efflux ratio (B→A)/(A→B)	mouse liver microsome stability ($T_{1/2}$)	PBS-pH 7.4 Stability: % remaining after 48h	Mouse plasma stability: % remaining after 48h
NCGC00037850	35.9 μ M	21	0.68	< 10min.	100	98

Note: kinetic solubility analyses was performed by Analiza Inc. and are based upon quantitative nitrogen detection as described (www.analiza.com). The data represents results from three separate experiments with an average intraassay %CV of 4.5%. LogD analysis was performed by Analiza Inc. and are based upon octanol/buffer portioning and quantitative nitrogen detection of sample content as described (www.analiza.com). All other data were conducted at Pharmaron Inc.

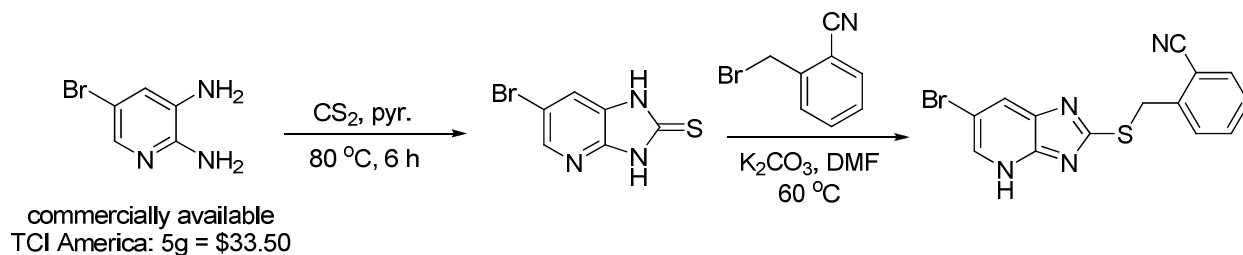


Buffer Stability (48 h @ 25°C) of (NCGC00037850/CID:2331284/MLS002729013/ML149), Percent remaining after 48h = 100%:

2.3 Probe Preparation

ML147:

Scheme 1: Synthetic route to (NCGC00044151-02/CID:3245059/MLS002729015/ML147):



The synthesis of the probe molecule was achieved in two steps from the commercially available 5-bromopyridine-2,3-diamine, as shown in Scheme 1. The first step involved cyclization to 6-bromo-1H-imidazo[4,5-b]pyridine-2(3H)-thione using carbon disulfide and pyridine as the solvent, followed by acidification as described previously². Alkylation of the sulfur moiety with the requisite substituted benzyl bromide was accomplished using potassium carbonate in DMF at 60°C to afford the desired molecule. The final product was purified using reversed-phase

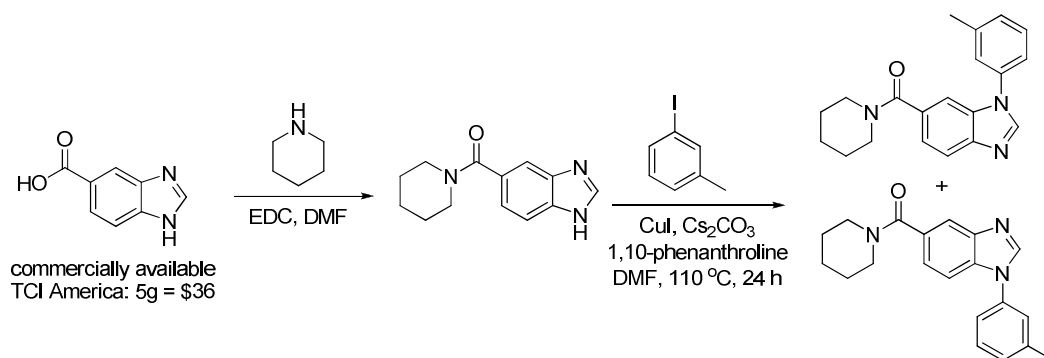
preparative HPLC. Additional analogues could be rapidly synthesized by either changing the diamine or benzyl halide starting material.

General procedure for the preparation of 6-bromo-1H-imidazo[4,5-b]pyridine-2(3H)-thione: CS₂ (10equiv) was added to a solution containing 5-bromopyridine-2,3-diamine (1equiv) in pyridine; the reaction was heated to 80°C and stirred at this temperature for 6 h. After this time, the reaction was poured into ice water and the precipitated solid was collected by filtration. This solid was carried through crude to the next reaction.

General procedure for the preparation of 2-((6-bromo-4H-imidazo[4,5-b]pyridin-2-ylthio)methyl)benzonitrile (CID: 3245059): 2-cyano benzyl bromide (1.1equiv) was added to a solution of crude 6-bromo-1H-imidazo[4,5-b]pyridine-2(3H)-thione (1equiv) in DMF, followed by potassium carbonate (2equiv). The reaction mixture was heated to 60°C for 5 h, and then cooled to room temperature, filtered, and the crude DMF solution submitted for purification via reversed-phase prep HPLC.

ML148:

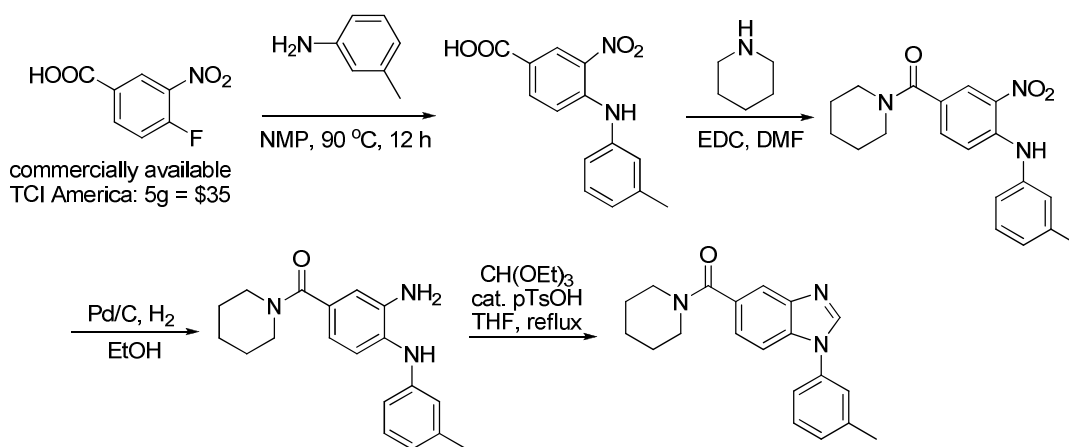
Scheme 2: Initial Synthetic route to (NCGC00065167-02/CID:3243760/MLS002729014/ML148):



Initial attempts to resynthesize (and confirm) our lead compound CID: 3243760 involved formation of the requisite amide using EDC coupling conditions with 5-benzimidazolecarboxylic acid and piperidine. Construction of the N-aryl linkage was achieved using a variety of conditions, including using a Buchwald coupling¹³ with 1-iodo-3-methylbenzene in the presence of copper iodide, cesium carbonate and 1,10-phenanthroline in DMF at elevated temperatures, as shown above. Additionally, Suzuki-coupling conditions using the requisite boronic acid in a copper acetate catalyzed reaction were attempted. Unfortunately, while both reactions gave some

of the desired product, the product ratio of the formed regioisomers was never greater than 1:1. Also, they could not be efficiently separated by either normal phase column chromatography or reversed-phase HPLC. There was the additional concern that even if the products could be separated, it may be difficult to unequivocally determine which was the desired regioisomer in the absence of an X-Ray structure or an advanced NMR technique. As such, we pursued an alternate route as shown below, which consisted of more steps, yet left no doubt as to the proper structural assignment.

Scheme 3: Synthetic route to (NCGC00065167-02/CID:3243760/MLS002729014/ML148):



In this alternate route, the first step involved nucleophilic displacement of the aromatic fluoride on 4-fluoro-3-nitrobenzoic acid with 3-methylaniline using NMP as the solvent at 90°C for 12 h. Formation of the amide proceeded smoothly using standard conditions (EDC, DMF). Subsequent reduction of the aromatic nitro group via hydrogenation with Pd/C, H₂ gave the desired aromatic diamine in high yield. Finally, acid catalyzed cyclization using triethylorthoformate in the presence of pTsOH in THF at reflux gave the desired benzimidazole product in high yield¹⁴. Again, while this route is not amenable to a parallel library synthesis, it provided the lead probe compound in large quantities with an unequivocal assignment of structure/regiochemistry.

General procedure for the preparation of 3-nitro-4-(m-tolylamino)benzoic acid: m-toluidine (1 equiv) was added to a solution containing 4-Fluoro-3-nitrobenzoic acid (1equiv) in NMP (2 ml/mmol); the reaction was heated to 90°C and stirred at this temperature for 12 h. After this time, the reaction was cooled to room temperature and poured into ice water and the precipitated

solid was collected by filtration and washed with water. This solid was carried through crude to the next reaction.

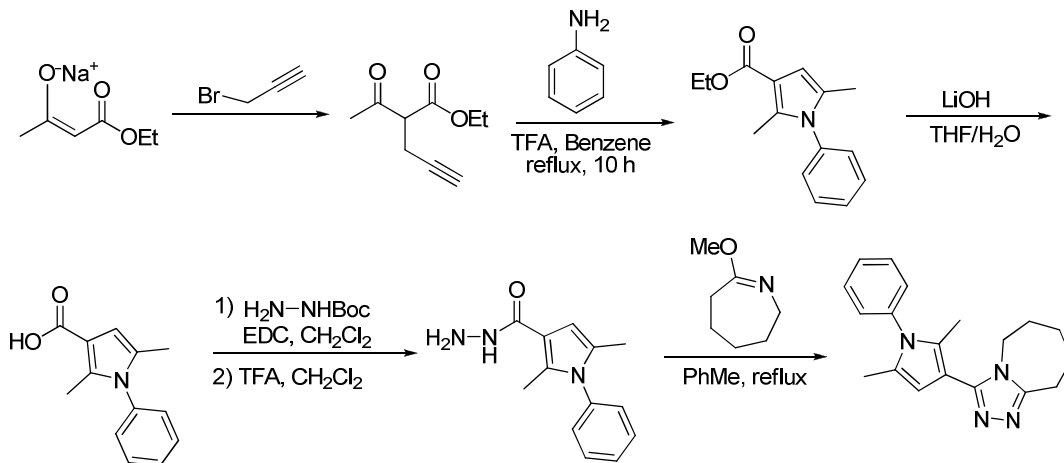
General procedure for the preparation of (3-nitro-4-(m-tolylamino)phenyl)(piperidin-1-yl)methanone: Piperidine (1.1equiv), followed EDC (1.2equiv), was added to a solution of crude 3-nitro-4-(m-tolylamino)benzoic acid (1equiv) in DMF (3 ml/mmol). The reaction mixture was stirred at room temperature for 2 h, then diluted with ethyl acetate and washed with water and brine. The collected organic layer was dried (MgSO₄), filtered and concentrated under reduced pressure. The crude product was purified on a Bitoage® SP1 system using hexane/ethyl acetate as the mobile phase.

General procedure for the preparation of (General procedure for the preparation of (3-amino-4-(m-tolylamino)phenyl)(piperidin-1-yl)methanone: Pd/C was added to a solution containing (3-nitro-4-(m-tolylamino)phenyl)(piperidin-1-yl)methanone (10 mmol) in ethanol (3 ml/mmol) and the reaction was allowed to stir under H₂ (1 atm) overnight. After this time, the solution became colorless. The reaction mixture was filtered through celite and concentrated under diminished pressure. The resulting solid did not require additional purification and was used directly in the next step.

General procedure for the preparation of piperidin-1-yl(1-m-tolyl-1H-benzo[d]imidazol-5-yl)methanone (NCGC00065167-02/CID:3243760/MLS002729014/ML148): Trimethyl orthoformate (3equiv), followed by cat. pTsOH, was added to a solution containing (3-amino-4-(m-tolylamino)phenyl)(piperidin-1-yl)methanone (1equiv) in THF (3 ml/mmol). The solution was heated to reflux and stirred overnight, after which time LC/MS monitoring of the reaction revealed complete consumption of the starting material. The excess solvent was removed under diminished pressure and the crude solid was dissolved in DMSO and submitted for purification via reversed-phase HPLC.

ML149:

Scheme 4: Initial Synthetic route to (NCGC00037850-02/CID:2331284/MLS002729013/ML149):



The synthesis of CID: 2331284 commenced with the preparation of ethyl 2-acetyl-4-ynopentanoate, as shown above. Typical procedures involve treatment of ethyl acetoacetate with sodium hydride, followed by addition of propargyl bromide¹⁵. However, we chose to use the readily available sodium salt of ethyl acetoacetate, which when reacted with propargyl bromide at room temperature in THF, gave the desired product in high yield. Formation of the 1,2,3,5-substituted pyrrole was accomplished by treatment with aniline in the presence of 1eq. of TFA in benzene at reflux, which results in amination of the carbonyl and subsequent 5-exo-dig cyclization of the enaminone, followed by aromatization¹⁶. Attempts to form the required hydrazine directly from the ethyl ester failed (hydrazine in Ethanol at reflux for extended periods), so the ester was saponified using LiOH to provide the carboxylic acid intermediate in good yield. Amidation with Boc-hydrazine using EDC-mediated coupling conditions, followed by deprotection of the Boc group using TFA, gave the hydrazide. Treatment of the acyl hydrazine with the commercially available imino ether in toluene at reflux gave the desired triazole in good yield¹⁷. If other non-commercially available imino ethers are desired, they could be rapidly prepared starting from the requisite lactam using Meerwein's salt.

General procedure for the preparation of ethyl 2-acetyl-4-ynopentanoate: Propargyl bromide (1.1equiv) was added to a solution containing the sodium salt of ethyl acetoacetate (1equiv) in THF (3 ml/mmol); the reaction was stirred at room temperature for 6 h. After this time the

reaction mixture was concentrated under reduced pressure and purified on a Bitoage® SP1 system using hexane/ethyl acetate as the mobile phase to give the desired product.

General procedure for the preparation of ethyl 2,5-dimethyl-1-phenyl-1H-pyrrole-3-

carboxylate: TFA (1 equiv) was added to a solution of ethyl 2-acetylpent-4-ynoate (1 equiv) and aniline (1.1 equiv) in benzene (3 ml/mmol). The reaction mixture was heated to reflux and stirred overnight, then cooled to room temperature and concentrated under diminished pressure. The crude residue was purified on a Bitoage® SP1 system using hexane/ethyl acetate as the mobile phase to give the desired product.

General procedure for the preparation of 2,5-dimethyl-1-phenyl-1H-pyrrole-3-

carbohydrazide: LiOH (10equiv) was added to a solution containing ethyl 2,5-dimethyl-1-phenyl-1H-pyrrole-3-carboxylate (1equiv) in THF/H₂O (3:1) (2 ml/mmol), and the reaction mixture was warmed to 60°C and stirred until consumption of the starting material (~3 h). After this time, the reaction was cooled to room temperature and diluted with ethyl acetate and washed with water and brine. The organic layer was separated, dried (MgSO₄), filtered and concentrated under reduced pressure. The resulting acid was pure enough to be used directly in the next step. This acid (1equiv) and Boc-hydrazide (1.2equiv) was dissolved in CH₂Cl₂ (3 ml/mmol) and EDC (1.3equiv) was added. The reaction mixture was stirred at room temperature for 1 h, at which time, LC/MS analysis revealed consumption of the starting material. The reaction mixture was diluted with CH₂Cl₂ and washed with water and brine. The organic layer was separated, dried (MgSO₄), filtered, concentrated under diminished pressure, and then placed on the high vacuum overnight.

General procedure for the preparation of (NCGC00037850-

02/CID:2331284/MLS002729013/ML149): Commercially available (*E*)-7-methoxy-3,4,5,6-tetrahydro-2H-azepine (1.1equiv) was added to a solution containing 2,5-dimethyl-1-phenyl-1H-pyrrole-3-carbohydrazide (1 equiv) in toluene (3 ml/mmol). The solution was heated to reflux and stirred overnight, after which time LC/MS monitoring of the reaction revealed complete consumption of the starting material. The excess solvent was removed under diminished pressure and the crude solid was dissolved in DMSO and submitted for purification via reversed-phase HPLC.

3 Results

Please see subsections for detailed results.

3.1 Summary of Screening Results

A qHTS of 150,839 samples across 895 plates resulted in a high average Z' of 0.86 (Figure 1a). The intra-plate control of Sigma G-6416 had an average IC_{50} of $10.42\mu M$ with an MSR of 1.5 (Figure 1b). Each sample's readout was captured in a kinetic mode with multiple reads per well, including the first background fluorescent read. This robust and stable screen resulted in a large high quality concentration-response dataset that yielded inhibitors with potencies ranging from $<100nM$ to $>57\mu M$.

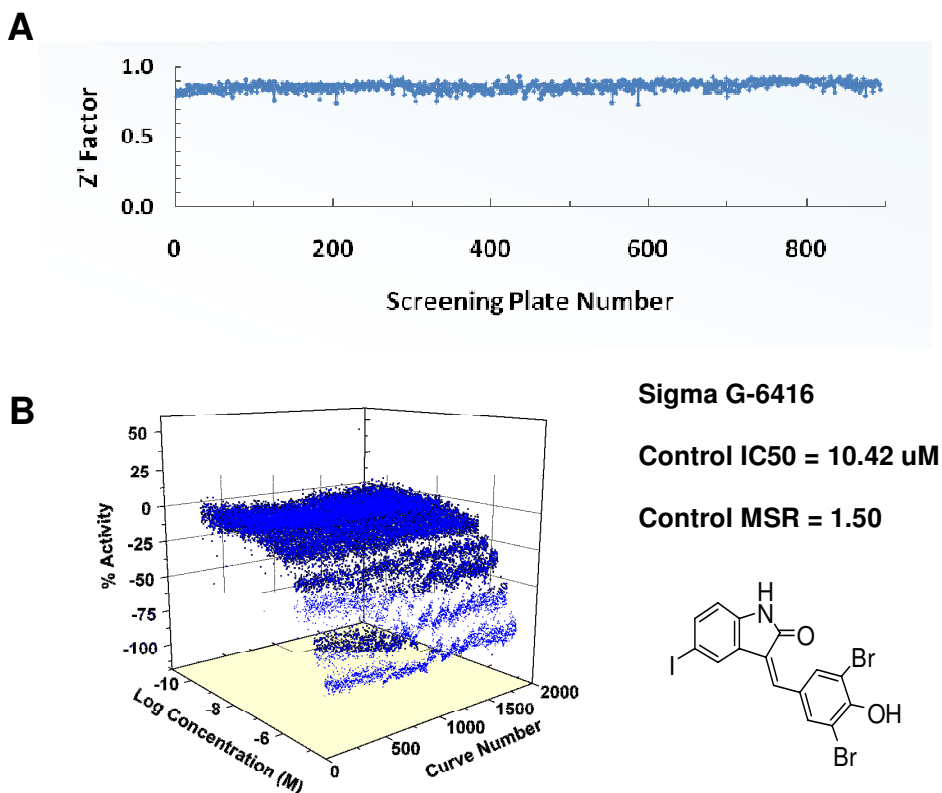


Figure 1. Plate and control performance of HPGD primary screen

Identification of lead

The primary screen resulted in a large number of potential inhibitors (Figure 2). Data was analyzed as described before¹⁰. A total of 24,226 (16%) samples gave significant concentration-dependent response. The first kinetic read for each sample was used to flag compounds that showed high background fluorescence. The delta kinetic read calculations for such inactive samples could lead to a concentration-dependent response due to compound fluorescence rather than putative inhibition. This helped eliminate 13,247 (8.77%) of actives. Additionally, 4,483 (2.97%) compounds had weak response curves with 40% or less inhibition at the top tested concentration of 57 μ M. The remaining 6,496 actives were further filtered by potency, and a total of top 89 samples spanning 23 chemical clusters and 15 singletons were chosen for follow up in the confirmatory screen and the thermal shift secondary assay.

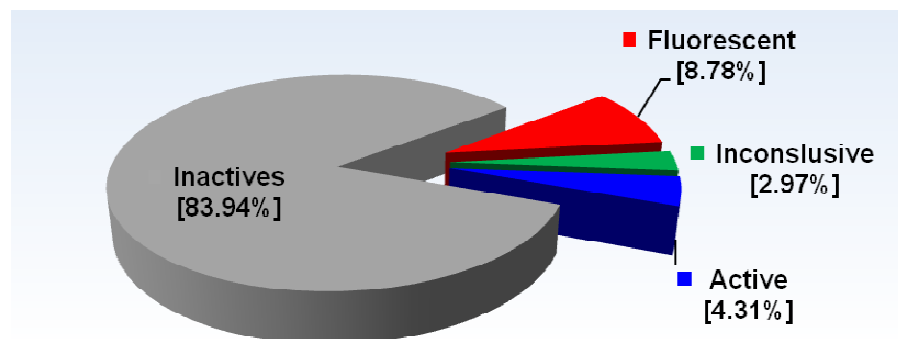


Figure 2. Activity categorization of 150,839 samples screened against HPGD

3.2 Dose Response Curves for Probe

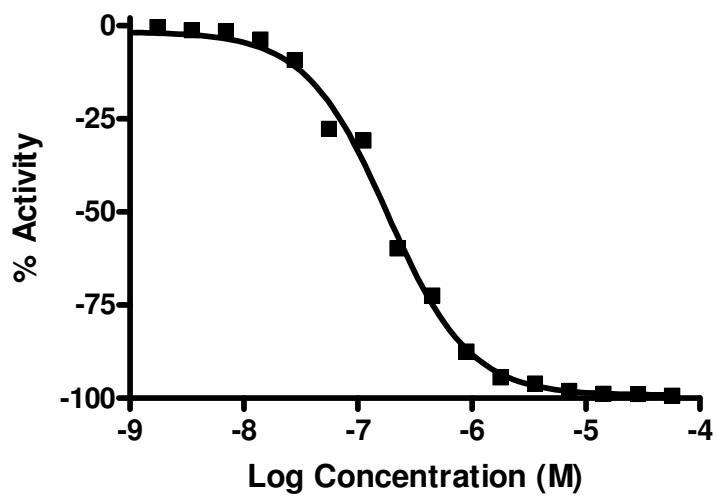


Figure 3. Dose response curve of ML147 in primary screen assay.

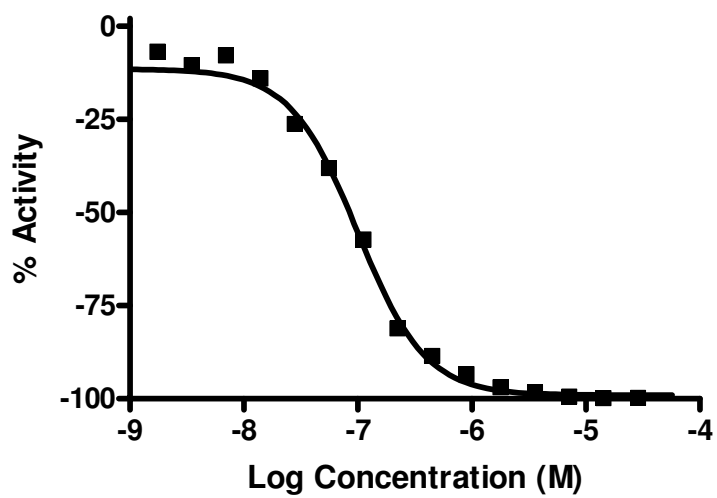


Figure 4. Dose response curve of ML148 in primary screen assay.

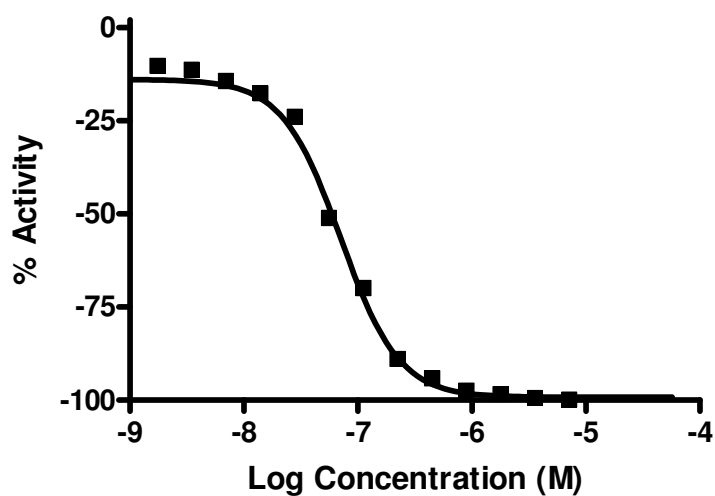


Figure 5. Dose response curve of ML149 in primary screen assay.

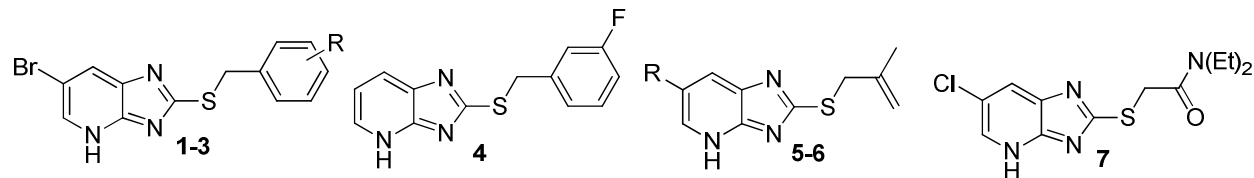
3.3 Scaffold/Moiety Chemical Liabilities

While many of the series found in the qHTS contained reactive functional groups, the series chosen for probe development did not contain any serious liabilities.

3.4 SAR Tables

ML147:

Table 1: SAR of 15-HPGD Inhibition

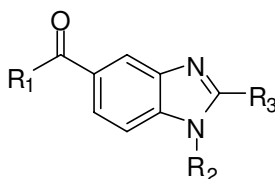


Analogue	CID	SID	R	IC ₅₀ (μM) ^a
1	3245059	99343744	2-CN	0.141
2	882270	7838872	2-F	0.63
3	708453	14739715	4-F	0.63
4	573334	14725914	NA	17.8
5	2039561	14742792	Cl	12.5
6	665481	50431841	H	22.3
7	665534	864287	NA	12.6

^a Note: all IC₅₀ values represent the average of three experiments (n = 3). When tested in collaborator's assay, an IC₅₀ of 25nM was determined for the probe compound with an estimated K_i of 5nM.

ML148:

Table 2: SAR of 15-HPGD Inhibition

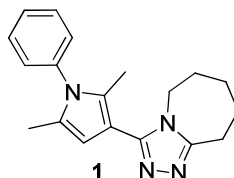
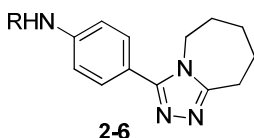
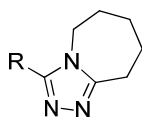
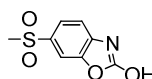
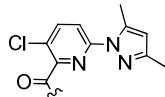
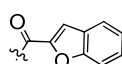
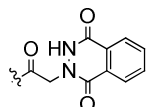
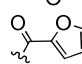
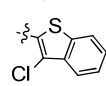
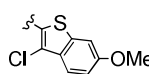
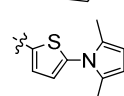


Analogue	CID	SID	R ₁	R ₂	R ₃	IC ₅₀ (μM) ^a
1	3243760	99343745	piperidine	3-Me-Ph	H	0.056
2	2999763	3716805	3-Me-piperidine	H	H	1.99
3	3239407	3239407	morpholine	4-OMe-Ph	Me	2.23
4	3238792	4244157	(CH ₂) ₂ OMe	3,4-F-Ph	H	2.5
5	3244293	4250491	(CH ₂) ₂ OMe	3-F-Ph	Me	7.10
6	3241847	4247671	1,4-dioxo-8-azaspiro[4.5]decane	3-F-Ph	Me	2.8
7	3245103	4251412	1,4-dioxo-8-azaspiro[4.5]decane	cyclohexyl	H	7.9
8	3241262	4246991	furfurylamine	4-OMe-Ph	Me	8.9
9	3245536	4251909	furfurylamine	2-OMe-Ph	H	12.5

^a Note: all IC₅₀ values represent the average of three experiments (n = 3). When tested in collaborator's assay, an IC₅₀ of 7.6nM was determined for the probe compound.

ML149:

Table 3: SAR of 15-HPGD Inhibition

				
1	2-6	6-12		
Analogue	CID	SID	R	IC50 (μM) ^a
1	2331284	99343743	NA	0.089
2	2997804	3711888		0.126
3	2120850	3713175		1.77
4	2089578	22407945		2.24
5	2523478	16952888		3.54
6	2359122	22405790		8.91
7	2414986	3717002		1.99
8	2414965	3717353		1.0
9	2341870	3717829		3.16
10	853732	14744353	4-Me-Ph	5.01
11	658120	856762	3-Br-Ph	6.31
12	745476	14731869	4-Br-Ph	7.07

^a Note: all IC₅₀ values represent the average of three experiments (n = 3). When tested in collaborator's assay, an IC₅₀ of 15nM was determined for the probe compound.

3.5 Cellular Activity

No cellular activity was assessed for ML147, for ML148 and 3; however, Caco2 permeability data (shown above) shows this compound is very cell permeable and has an efflux ratio of ~0.5 and ~1 respectively. This data suggests that these compounds would be suitable tool compounds with which to investigate the effects of HPGD in a cellular context.

3.6 Profiling Assays

These probe compounds have been tested in 459, 501, and 507 assays respectively for ML147, 2, and 3 (PubChem), and has thus far, they have only been active in HPGD-related assays performed at NCGC. Specifically, these compounds are also inactive against a related dehydrogenase, ALDH1A1, with no inhibition observed at $> 57\mu\text{M}$ for ML147 and inactivity against related dehydrogenases, HADH2 and HSD17 β 4, with no inhibition observed at $> 57\mu\text{M}$ for probes 2 and 3.

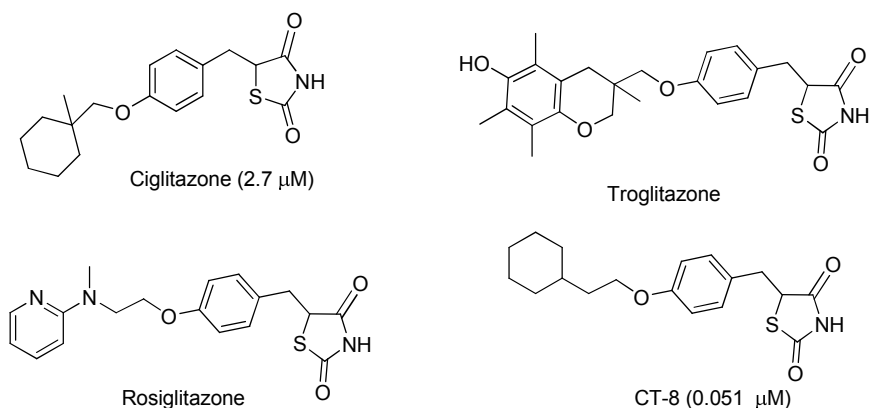
4 Discussion

One of the advantages of our qHTS screening platform is the ability to generate SAR directly from the primary screen, as shown in Table 2. Accordingly, we discovered a highly potent molecule [**CID: 3243760, ML148**: $IC_{50} = 56.2$ nM (qHTS data)] which exceeded the predetermined probe criteria by 20-fold (criteria: $1\mu M$), and subsequent testing in a 384 well-based screen in the assay provider's lab revealed an IC_{50} of 7.9nM for the resynthesized probe. The SAR seems to indicate a strong preference for the piperazine amide, as other amides were not well tolerated. Moreover, addition of a methyl group at the 2-position appears unfavorable, as does other N-arylation products. While the complete SAR picture is not fully understood, the combination of the potency and drug-like nature of this scaffold suggested no further need for engaging additional chemistry efforts. However, following our typical protocol, we did utilize in-house chemistry resources to resynthesize the top lead for confirmation of the structure and activity. Additionally, mechanism of action studies indicate that this chemotype inhibits HPGD in a *noncompetitive fashion*, which differed from the 2-((6-bromo-4H-imidazo[4,5-b]pyridin-2-ylthio)methyl)benzonitrile probe molecule (see Related Probes CID: 3245059) which displayed *competitive* inhibition. These combined attributes lead us to the selection of this molecule as the probe candidate.

The potencies of our top molecules were 89nM in the qHTS assay and 15.0nM in the secondary thermal shift assay. These values represent the activity of the *synthesized* version of the compound and represent a 10-100-fold lower IC_{50} than the predetermined probe criteria. Additionally, this was the second of two chemotypes which displayed non-competitive inhibition of HPGD (see Related Probes). However, it represents a much different chemical scaffold, providing another useful and novel probe molecule for the scientific community. Since the predefined probe criteria had been met out of the primary screen, additional in-house chemistry resources to further improve the potency were not required. At the time of project completion, the assay provider no longer had resources to continue pursuing this project. For this reason, we submitted an extended characterization proposal in hopes of providing funds for additional biological characterization and medicinal chemistry optimization of this promising lead compound. The SAR table 1 shown above highlights some of the nascent SAR from the primary screen of the probe and its similar compounds. It appears that a phenyl sulfonamide is well

tolerated in place of the phenyl pyrrole, as similar activity was observed (**1** = 89nM, **2** = 126nM). However, replacing the sulfonamide moiety with an amide functionality seems less desirable, as most of those analogues were in the low micromolar range. Additionally, direct substitution of other heterocycles and phenyl derivatives to the triazole also seem unfavorable. One could explore different cycle rings as part of the triazole core and/or explore analogues of the phenyl ring attached to the pyrrole to pick up additional potency and/or improve pharmacokinetic properties if required

4.1 Comparison to existing art and how the new probe is an improvement



Several types of ligands for HPGD, including activators and inhibitors, have been identified previously. These include clinically approved neuroactive drugs like imipramine and chlorpromazine, which apparently weakly activate the enzyme; non-steroidal anti-inflammatory drugs (NSAIDs) and COX inhibitors, e.g. indomethacin, sulindac, and niflumic acid; or peroxisome proliferator-activated receptor gamma agonists, such as thiazolidinediones (Ciglitazone, Troglitazone and Rosiglitazone), which weakly inhibit HPGD in the micromolar ranges¹⁹. Recently, a related thiazolidinedione, CT-8, and analogs were reported to have potencies ranging from 0.030 μM – 2 μM ¹⁹. However, there is no mention of selectivity, and given the known and seemingly unrelated antidiabetic effects of this class of compounds, these likely do not represent acceptable probe molecules. In contrast, the probe identified here is a potent and competitive 141nM HPGD inhibitor (26nM in collaborator's assay) that is also selective against a related dehydrogenase, ALDH1A1. In summary, the probes and their series

identified here provide the research community a best-in-class selective inhibitor series for HPGD²⁰.

4.2 Mechanism of Action Studies

Differential Scanning Fluorimetry (also termed thermal shift) studies to assess the stability of human 15-PGDH in presence of compounds were performed as described before, with variations. In brief, the protein was diluted to a final assay concentration of 1 μ M in 100mM Tris buffer, pH 8.0, containing 0.01% Tween-20 and 1:1000 SYPRO orange dye. The final assay volume was 10 μ l, with or without 200 μ M of either NAD⁺ or NADH. Compounds were added 1:5 from appropriate stock solutions in 10% (v/v) DMSO to comprise either 50 or 250 μ M final concentrations. Heat denaturation curves were recorded using a RT-PCR instrument (Mx3005p, Agilent) applying a temperature gradient of 2°C/min. Analysis of the data was performed using DSF Analysis vers. 2.5 (<ftp://ftp.sgc.ox.ac.uk/pub/biophysics>) and Prism 5.0 (GraphPad Software, Inc.). Of the confirmed follow-up actives, 3 top compounds that showed the most significant thermal stabilization of 15-PGDH were chosen for IC₅₀ determination (AID 2427). In presence of NAD⁺, a strong stabilization, which is expressed as the shift in the transition midpoint temperature (ΔT_m), was observed for the probe. Interestingly, we observed weak stabilization in the presence of NADH. An IC₅₀ of 26.4 nM was determined for the re-synthesized compound, while the purified re-purchased dry powder gave an IC₅₀ of 35.6 nM. Interestingly, we observed weak stabilization in the presence of NADH for ML147. In the presence of either NAD⁺ or NADH, a strong stabilization, which is expressed as the shift in the transition midpoint temperature (ΔT_m), was observed for Probes 2 and 3. For ML148, an IC₅₀ of 7.9nM was determined for the resynthesized compound, while the purified re-purchased dry powder gave an IC₅₀ of 4.3nM. For ML149, using a 384 well-based screen similar to the primary qHTS, an IC₅₀ of 15.0nM was determined for the re-synthesized compound, while the purified re-purchased dry powder gave an IC₅₀ of 9.3nM.

Table 4. ML147: Effect of probe compound on stability and activity of HPGD

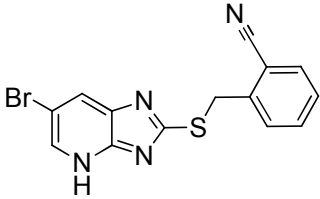
Probe Compound	Stabilization (ΔT_m) [°C]			Dose-response	
	w/o cofactor	NAD ⁺	NADH	Max. inhibition [%]	Retested IC ₅₀ [nM]
 <p style="text-align: center;">1</p>	-1.2 ± 1.1	12.2 ± 0.1	2.9 ± 0.5	100	35.6 ± 2.5 (re-purchased) 26.4 ± 2.4 (re-synthesized)

Table 5. ML148: Effect of probe compound on stability and activity of HPGD

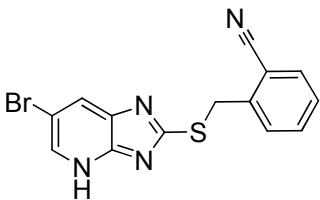
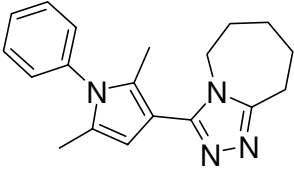
Probe Compound	Stabilization (ΔT_m) [°C]			Dose-response	
	w/o cofactor	NAD ⁺	NADH	Max. inhibition [%]	Retested IC ₅₀ [nM]
 <p style="text-align: center;">1</p>	-1.2 ± 1.1	12.2 ± 0.1	2.9 ± 0.5	100	35.6 ± 2.5 (re-purchased) 26.4 ± 2.4 (re-synthesized)

Table 6. ML149: Effect of probe compound on stability and activity of HPGD

Probe Compound	Stabilization (ΔT_m) [°C]			Dose-response	
	w/o cofactor	NAD ⁺	NADH	Max. inhibition [%]	IC ₅₀ [nM]
 1	0.1 ± 0.0	5.0 ± 0.1	10.5 ± 0.6	100	9.3 ± 0.7 (re-purchased) 15.0 ± 1.2 (re-synthesized)

In order to further investigate the mechanism-of-action for these probes, we performed extensive kinetic characterization in experiments with titration of the 15-PGDH substrate PGE₂ and of the co-substrate NAD, respectively. The addition of the probe inhibitor at increasing concentrations to the substrate titration caused an increase in K_m for PGE₂, suggesting competition of the inhibitor with the substrate for ML147 (Figure 6), and uncompetitive inhibition for ML148 and ML149 (Figure 7 and Table 7, respectively).

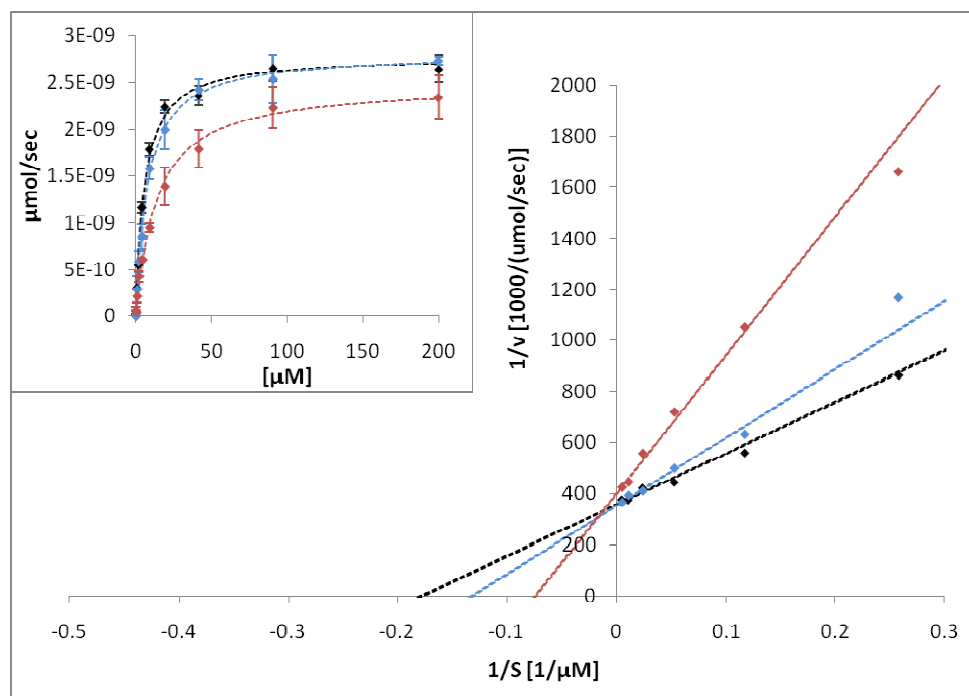


Figure 6. Mechanism-of-action studies of probe compound with respect to the substrate. Insets show the Michaelis-Menten graphs of 15-PGDH activity at increasing concentrations of PGE₂, while the main graphs show plots of the data after Lineweaver and Burk. Dotted lines in both representations show fits to the Michaelis equation. Black represents no inhibitor, blue denotes 10nM probe compound, and red denotes 50nM probe compound.

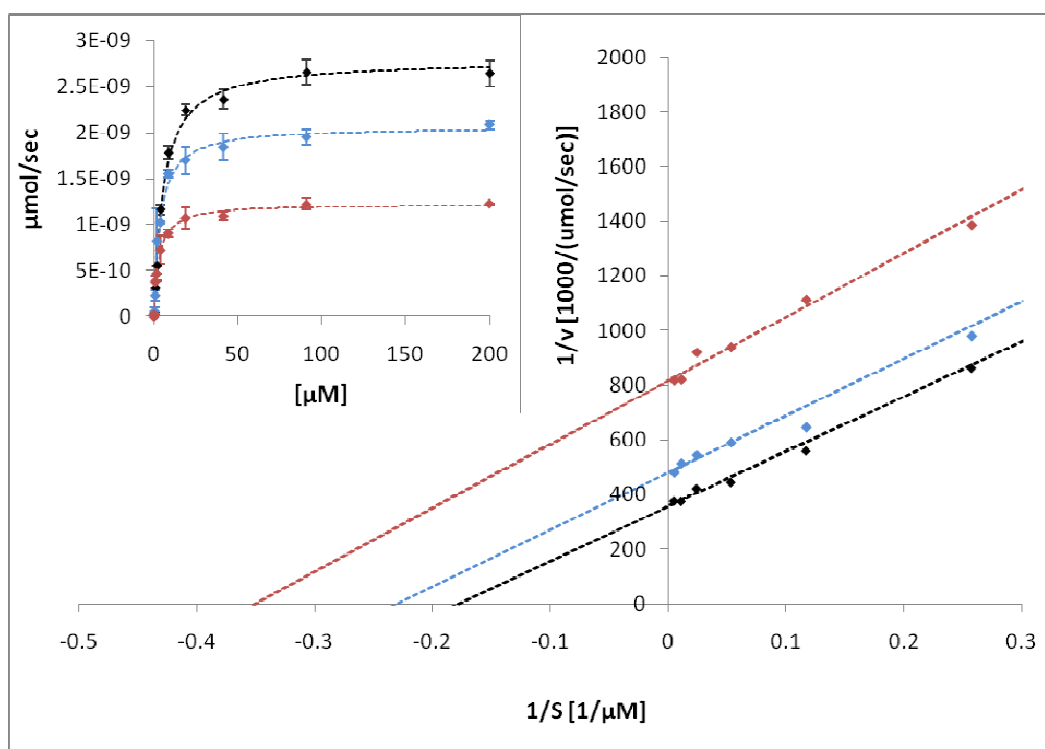


Figure 7. Mechanism-of-action studies of probe compound with respect to the substrate. Insets show the Michaelis-Menten graphs of 15-PGDH activity at increasing concentrations of PGE₂, while the main graphs show plots of the data after Lineweaver and Burk. Dotted lines in both representations show fits to the Michaelis equation. Black represents no inhibitor, blue denotes 10nM probe compound, and red denotes 50nM probe compound.

Table 7. Investigation of the mechanism of action for CID: 2331284.

	Conc. [nM]	Titration of PGE ₂				Titration of NAD ⁺			
		<i>K_m</i> [μM]	<i>V_{max}</i> [μ mol/ (min×mg)]	<i>k_{cat}</i> [1/sec]	<i>k_{cat}/K_m</i> [×10 ⁶]	<i>K_m</i> [μM]	<i>V_{max}</i> [μmol/ (min×mg)]	<i>k_{cat}</i> [1/sec]	<i>k_{cat}/K_m</i> [×10 ⁶]
CID: 2331284	4.0	5.6 ± 1.1	22.8	11.1 ± 0.5	2.0	n.d.	n.d.	n.d.	n.d.
	10.0	6.4 ± 0.6	15.4	7.5 ± 0. 2	1.2				
PGE ₂		5.5 ± 0.6	28.1	13.6 ± 0.3	2.5				
NAD ⁺						15.8 ± 0.9	21.2	10.3 ± 0.1	0.7

4.3 Planned Future Studies

Future studies for the ML147 probe project will include a thorough expansion of the SAR around this chemotype and investigation of the *in vitro* ADME properties. While the compound has an IC₅₀ value over 10-fold the aqueous solubility, we would look to improve the overall solubility of this compound through additional lead optimization work. We will also look to explore additional selectivity against other anti-targets such as HADH2 and HSD17β4.

Future studies for ML148 and ML149 projects will include a thorough expansion of the SAR around these chemotypes and investigation of the *in vitro* ADME properties. Unlike our previous competitive probe molecule which had limited aq. solubility, this compound has very favorable solubility.

5 References

1. Sheng, H., *et al.* Modulation of apoptosis and Bcl-2 expression by prostaglandin E2 in human colon cancer cells. *Cancer Res.* **1998**; 58, 362-366.
2. Buczynski, M.W., Dumlao, D. S., Dennis, E. A. Thematic Review Series: Proteomics. An integrated omics analysis of eicosanoid biology. *J. Lipid Res*, **2009**, 50, 1015-1038.
3. FitzGerald, G.A., COX-2 and beyond: Approaches to prostaglandin inhibition in human disease. *Nat. Rev. Drug Discov.* **2003**, 2, 879-890.
4. Tai, H.H., *et al.*, Prostaglandin catabolizing enzymes. *Prostaglandins Other Lipid Mediat*, **2002**, 68, 483-493.
5. (a) Ensor, C.M., *et al.*, Cloning and sequence analysis of the cDNA for human placental NAD (+)-dependent 15-hydroxyprostaglandin dehydrogenase. *J. Biol. Chem.*, **1990**, 265, 14888-14891. (b) Ensor, C.M. and Tai, H. H. Bacterial expression and site-directed mutagenesis of two critical residues (tyrosine-151 and lysine-155) of human placental NAD(+)-dependent 15-hydroxyprostaglandin dehydrogenase. *Biochim. Biophys. Acta*, **1994**, 1208, 151-156.
6. Yan, M., *et al.* 15-Hydroxyprostaglandin dehydrogenase, a COX-2 oncogene antagonist, is a TGF-beta-induced suppressor of human gastrointestinal cancers. *Proc Natl Acad Sci U S A*. **2004**. 101(50): 17468-73.
7. Thirumangalakudi, L., Rao Vittal, H., Grammas, P. Involvement of PGE2 and PGDH but not COX-2 in thrombin-induced cortical neuron apoptosis. *Neurosci. Lett.* **2009**, 452, 172-175.
8. Johnstone, M. A. Hypertrichosis and increased pigmentation of eyelashes and adjacent hair in the region of the ipsilateral eyelids of patients treated with unilateral topical latanoprost. *Am. J. Ophthalmol.* **1997**, 124, 544-547.
9. Meklir, B., Joyce, N. C.; PGE2: a mediator of corneal endothelial wound repair in vitro. *Am. J. Physiol.* **1994**, 266, C269-275.
10. Gelse, K., Beyer, C. The prostaglandin E2 system: A toolbox for skeletal repair? *Arthritis and Rheumatism*, **2010**, editorial.

11. Inglese, J., *et al.* Quantitative high-throughput screening: A titration-based approach that efficiently identifies biological activities in large chemical libraries. *Proc Natl Acad Sci U.S.A.* **2006**, *103*, 11473-8.
12. Yutilov, M. T., Scertilova, I. A. Thionation of Imazopyridines. *Chem. Heterocycl. Compd.* **1988**, *24*, 653-658.
13. Antilla, J.C., Baskin, J.M., Barder, T. E., Buchwlad, S.L. Copper-diamine-catalyzed N-arylation of pyrroles, pyrazoles, indazoles, imidazoles, and triazoles. *J. Org. Chem.* **2004**, *69*, 5578-5587.
14. Trost, B. M., Rudd, M. T. Ruthenium-catalyzed cycloisomerization of diynols. *J. Am. Chem. Soc.* **2005**, *127*, 4763-4776. (b) Okuro, K.; Alper, H. Intramolecular and Intermolecular Mn(III) Induced carbon monoxide trapping reaction of alkynes with malonate and cyano ester units. *J. Org. Chem.* **1996**, *61*, 5312-5315.
15. NeuroSearch A/S. Benzimidazole Derivatives and their use for modulating the GABAA receptor complex. WO2007/65864, 2007.
16. Demir, A. S., Aybey, A., Kayalar, M. TFA catalyzed sequential amination/annulation/aromatization reaction of 2-propynyl-1,3-dicarbonyl compounds with amines. A new one-pot approach to functionalized pyrroles. *ARKIVOC*, **2005**, 105-116.
17. Olsen, S., *et al.*, Adamantyl triazoles as selective inhibitors of 11 β -hydroxysteroid dehydrogenase type 1. *Bioorg. Med. Chem. Lett.* **2005**, 4359-4362.
18. Cho, H., and Tai, H. H. *Prostaglandins Leukot Essent Fatty Acids* **2002**, *67*, 461-465.
19. Wu, Y., Tai, H.-H., Cho, H. Synthesis and SAR of thiazolidinedione derivatives as 15-PGDH inhibitors. *Bioorg. Med. Chem.* **2010**, *18*, 1428-1433.
20. Nielsen, F. H., Schultz, L., Jadhav, A., Bhatia, C., Guo, K., Maloney, D. J., Pilka, E. S., Wang, M., Oppermann, U., Heightman, T. D., Simeonov, A. High Affinity inhibitors of human NAD⁺-dependent 15-hydroxyprostaglandin dehydrogenase: mechanism of inhibition and structure-activity relationships. *PLoS ONE*, **2010**, *5* (11): e13719.